Research Article | Vol. 11, No. 11 / 1 Nov 2021 / Optical Materials Express 3627
Optical Materials EXPRESS

Determination of the refractive index modulation of PQ:PMMA holographic phase gratings over a large spectral range through a two-level approximation of the electric susceptibility

JULIAN GAMBOA,[1,4] TABASSOM HAMIDFAR,[1] JASON BONACUM,[2] AND SELIM M. SHAHRIAR[1,2,3,5]

[1]Department of ECE, Northwestern University, Evanston, IL 60208, USA
[2]Digital Optics Technologies, Rolling Meadows, IL 60008, USA
[3]Department of Physics and Astronomy, Northwestern University, Evanston, IL 60208, USA
[4]JulianGamboa2023@u.northwestern.edu
[5]shahriar@northwestern.edu

Abstract: Phenanthrenequinone doped poly(methyl methacrylate) is a well-known holographic polymer used in many applications. It is important to consider the refractive index modulation (Δn) when designing a phase grating, as it heavily influences the diffraction efficiency. However, due to the behavior of the electric susceptibility in this material, the Δn will be different at varying reconstructed wavelengths. Here, we report on the observation of the difference in this modulation for various wavelengths. We develop a model for a two-level approximation of the electric susceptibility, based on the absorption spectrum of the material, to estimate the read wavelength dependence of the modulation for a given sample, and find our results to be in good agreement with this model.

1. Introduction

Holographic memory devices (HMDs) fall into two general categories: crystals and photopolymers, both of which have many uses in optical applications that require unique grating configurations. Crystals allow for high quality read-write holograms but tend to be extremely delicate and therefore difficult to implement in practical applications [1,2]. In contrast, photopolymers can be used for write-once read-many (WORM) configurations to create highly stable and long-lasting gratings [3,4]. These types of HMDs are useful for applications where reliability and longevity are key, but rewritability is not needed. One such medium is phenanthrenequinone-doped poly(methyl-methacrylate) (PQ:PMMA), which has been studied in detail by other authors [4–9] but is still in development for data storage and optical processing applications [10–13]. Recent efforts have focused on the development of a model for the exposure dynamics of the material based on the PQ's photo-induced reactions [14,15]. Such models are useful in the design stage of holographic devices, as they allow for simulations of varying parameters and characteristics. These models focus on the recording process but lack any insight into the post-recording light-matter interaction which dominates the reading process.

Holographic phase gratings are generated when two coherent beams of the same wavelength and polarization interfere with each other in a photosensitive medium, whereby the photo-induced reactions causes a permanent change in the refractive index [16,17]. In the case of PQ:PMMA, the difference in intensity between the peaks and troughs of the resulting interference pattern will cause different reactions in the photoreactive PQ dye that create a periodic modulation of the refractive index [4]. Once the hologram is written, only waves that meet the Bragg condition will diffract efficiently. If the reading beam has the same wavelength as that of the writing beam, then this occurs when the input angle matches that of either of the two writing beams. The

#440384 https://doi.org/10.1364/OME.440384
Journal © 2021 Received 19 Aug 2021; revised 21 Sep 2021; accepted 21 Sep 2021; published 4 Oct 2021

Optical Materials EXPRESS

diffracted beam then exits the hologram in the direction of the secondary writing beam [17]. This makes it possible to expose multiple holograms at the same location without interfering with one another by changing either the wavelength or input angle of the writing beams [18,19]. However, writing setups designed to multiplex through wavelength have the inherent problem of needing to supply multiple laser beams (one per desired wavelength) through the same beam path. Furthermore, such a system would only be able to write gratings for a limited range of wavelengths, where the photoreactive dye is most sensitive. For many applications, the read wavelengths fall in a spectral range that is not suitable for writing gratings in PQ:PMMA. Consider, for example, the case of monocular passive ranging, which measures light from an emissive source at three different wavelengths to estimate O_2 absorption along the beam path; Beer's law can then be used in conjunction with this data to estimate the distance from the source [20]. This application requires one measurement at 760nm and two additional measurements at surrounding wavelengths [10,21]. PQ:PMMA is not sensitive enough for writing in the NIR region [4], and so a different writing wavelength is required. Free space optical communication systems [10,22], multifocal microscopy [23], and spectroscopy [6,24] are other examples of applications that may benefit from holographic wavelength division multiplexing (WDM); for these cases also, the gratings have to be recorded at a wavelength that is different from the ones used in the applications.

This problem can be circumvented by designing a system that uses only one writing wavelength but generates gratings with the same k-vector that would result from the desired read wavelength at a given angle [7,8,10]. To do so, it is important to recall that the grating period, $|\vec{\Lambda}|$, is inversely proportional to the interference k-vector, $\vec{K} = \vec{K}_{W1} - \vec{K}_{W2}$, where the subscripts refer to the two write beams, as displayed in Fig. 1. The same k-vector can be achieved at a different wavelength of light by carefully controlling the beam angles [10,16,22]. Thus, both wavelengths can create the same grating. Moreover, one may arbitrarily choose the Bragg angle of the read beam at one wavelength (e.g., 1550 nm) and calculate the write angle at a distinct wavelength where the PQ is highly photosensitive (e.g., 532 nm). To design such a system optimally, one has to be able to predict how the sample operates at the desired wavelengths, by taking into account the electrical susceptibility of the material. This knowledge of wavelength dependence also allows for a single sample to be used for a wide range of applications.

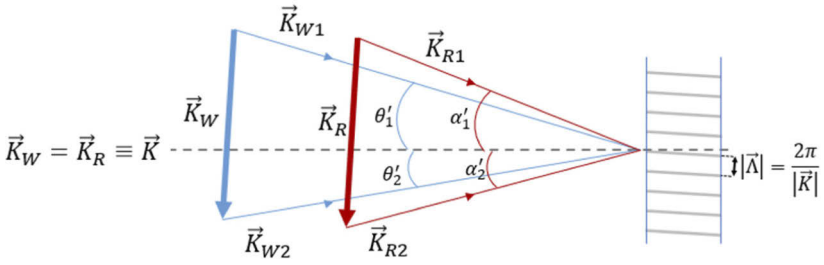

Fig. 1. K-vector diagram showing how two distinct wavelengths can generate the same grating. Here, the beams represented in blue have a shorter wavelength than the ones represented in red, but $\vec{K}_W$ and $\vec{K}_R$ are identical.

In the present study, we observe a non-trivial wavelength dependence of the refractive index modulation in unslanted PQ:PMMA gratings. To interpret this wavelength dependence, we construct a two-level light-matter interaction model and derive a wavelength dependent equation for the refractive index modulation, which incorporates the behavior of the electrical susceptibility. The parameters of the model were obtained from the measurement of the absorption spectrum of exposed PQ:PMMA. The model also includes a coefficient for the density modulation that is unique to each fabricated sample and is determined experimentally. The variation of the

Optical Materials EXPRESS

refractive index modulation predicted by this model is in good agreement with our measurements at read wavelengths of 532 nm, 780 nm, 1300 nm, and 1550 nm.

2. Two-level approximation of the electrical susceptibility of PQ:PMMA

PQ:PMMA gratings are formed from the reaction between PQ dye molecules and MMA monomers when exposed to light during the writing process [4], which changes the volumetric density of PMMA/MMA across the sample according to the interference between the two write beams. This can be written as a sinusoidal modulation around an average density:

$$\rho = \rho_0 + \rho_m \cos(\vec{K} \cdot \vec{R}) \tag{1}$$

where ρ_0 and ρ_m are the amplitudes of the initial and modulated density, respectively, $\vec{K}$ is the grating vector, and $\vec{R} = (x, y, z)$ is the position vector. After writing and post-processing, the density is frozen and can be considered to be static.

We model each molecule of the material after exposure as a simple two-level system that absorbs light most efficiently at its resonant frequency, $\omega_0 = 2\pi c/\lambda_0$, with a linewidth of Γ. The notation here follows that of section 2 in Ref. [25]. More general descriptions of two-level systems under various scenarios can be found in Ref. [26]. The electrical susceptibility, χ, of the material can be expressed as $\chi = \chi' + i\chi''$, where the real and imaginary parts are given by [27]:

$$\chi' = Re\{\chi\} = -\xi\rho \cdot \frac{8\delta}{\Gamma^2 + 2\Omega^2 + 4\delta^2} \tag{2}$$

$$\chi'' = Im\{\chi\} = \xi\rho \cdot \frac{4\Gamma}{\Gamma^2 + 2\Omega^2 + 4\delta^2} \tag{3}$$

Here, $\delta = \omega - \omega_0$ is the detuning of the read light applied at the frequency of ω, and Ω is the Rabi frequency. The parameter ξ is proportional to the mean dipole moment produced in each molecule when it is in an equal superposition of the ground and excited state and can be taken as a constant. Substituting expression (1) in (2), and considering that $|\delta|, \Gamma \gg \Omega$ for low intensity beams, we can write:

$$\begin{aligned} \chi' &\approx -\xi \cdot \frac{8\delta}{\Gamma^2 + 4\delta^2} \cdot (\rho_0 + \rho_m \cos(\vec{K} \cdot \vec{R})) \\ &= -\xi\rho_0 \cdot \frac{8\delta}{\Gamma^2 + 4\delta^2} - \xi\rho_m \cdot \frac{8\delta}{\Gamma^2 + 4\delta^2} \cos(\vec{K} \cdot \vec{R}) \end{aligned} \tag{4}$$

We now note that the real part of the electric susceptibility determines the refractive index 'n':

$$n = \sqrt{1 + \chi'} \tag{5}$$

For the case of PQ:PMMA between 532 nm and 1550 nm, both χ' and χ'' are assumed to be small, and as such we can approximate this square root with its Taylor series expansion and keep only the first two terms:

$$\begin{aligned} n &\approx 1 + \chi'/2 \\ &= 1 - \xi \cdot \rho_0 \frac{4\delta}{\Gamma^2 + 4\delta^2} - \xi\rho_m \cdot \frac{4\delta}{\Gamma^2 + 4\delta^2} \cos(\vec{K} \cdot \vec{R}) \end{aligned} \tag{6}$$

Finally, for the refractive index to form a grating, it must be of the form show in Eq. (1), and may be written as [16]:

$$n = n_0 + \Delta n \cos(\vec{K} \cdot \vec{R}) \tag{7}$$

Optical Materials EXPRESS

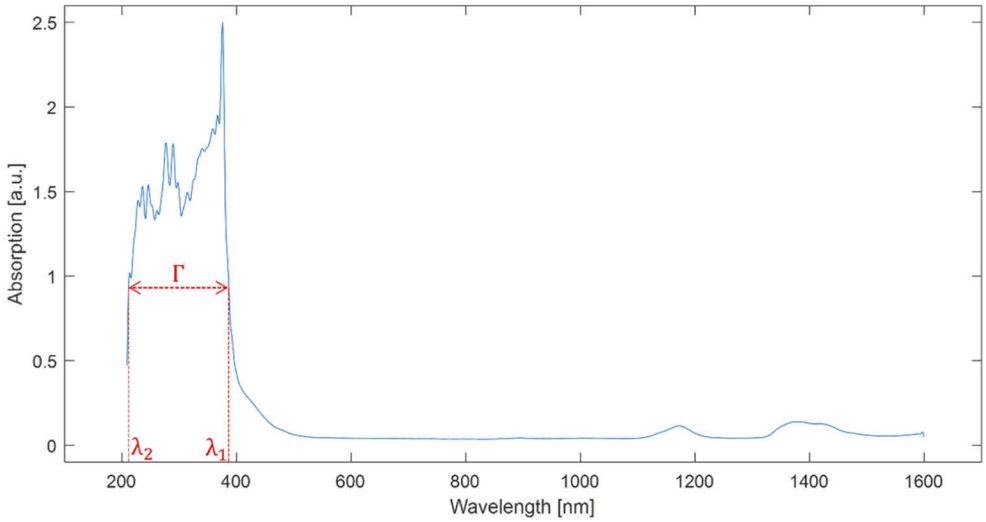

Fig. 2. UV-VIS-NIR absorption spectrum of a ~2mm thick sample of exposed PQ:PMMA as measured on a Perkin Elmer Lambda 1050 spectrophotometer through an integrating sphere.

Comparing (6) and (7), the refractive index modulation, Δn, can be expressed as:

$$\begin{aligned} \Delta n &\approx -\xi\rho_m \cdot \frac{4\delta}{\Gamma^2 + 4\delta^2} \\ &= -\alpha \cdot \frac{4\delta}{\Gamma^2 + 4\delta^2} \end{aligned} \tag{8}$$

where $\alpha = \xi\rho_m$. For any given grating, α and Γ will remain constant, but the δ term will depend on the wavelength of the reading beam. The α parameter contains information about the physical properties of a particular grating and will depend on the fabrication and writing parameters. It may be calculated from the measured value of Δn at a reference wavelength for any given grating. However, Γ depends only on the properties of the PQ:PMMA and can be determined by observing its absorption spectrum. We denote the center of the absorption spectrum by $\lambda_0 = (\lambda_1 + \lambda_2)/2$, and define λ_1 and λ_2 to be the wavelengths at the edges of the absorption signal, so that the linewidth can be expressed as $\Gamma = 2\pi c(\lambda_2^{-1} - \lambda_1^{-1})$.

In order to obtain these parameters, the absorption spectrum of a sample had to be measured. The sample used in this paper to test the model was a 50mm diameter disk fabricated as described in [4], using a free-space Bragg angle of 8.5° at the writing wavelength (532 nm), which yields a grating periodicity of 1.7996 μm. Twelve gratings measuring ~5 mm x 7 mm were created at different locations on the same sample with varying exposure energies. The thickness at each location was measured with a micrometer, with all of the values falling between 1.999 mm and 2.056 mm, with an average value of 2.027 mm and a standard deviation of 25.9 μm. The thickness of each individual location was used in the relevant calculations for its corresponding grating. Figure 2 shows the UV-VIS-NIR absorption spectrum of a single hologram in this sample after the writing process. The measurements were taken with a Perkin Elmer Lambda 1050 spectrophotometer through an integrating sphere with a spectral resolution of 1 nm. The measured spectrum is consistent with what has been presented by Hsiao et al. in Fig. 3 (graph corresponding to the exposed sample) of Ref. [4] over the UV-VIS region. One exception is a sharp but repeatable peak at ~375 nm. In addition, we see two smaller peaks in the NIR region, which was not covered in the aforementioned data presented by Hsiao et al. but agrees with the

Optical Materials EXPRESS

extended spectrum presented by Chung et al. in Fig. 1 of Ref. [28]. In our model, we consider primarily the broad resonance on the left, treating it as resulting from an effective two level system. For the wavelengths of interest, the effect of the peak at ~375 nm is expected to be negligible, due to the fact that it is very narrow. We also exclude the effect of the two resonances in the NIR region, since these are significantly smaller than the broad resonance on the left. In the future, we will modify our model to include the effects of these peaks, modeling each one of them as an additional two level system, and determine the degree to which these affect the diffraction properties for our wavelengths of interest.

From the broad resonance on the left edge of Fig. 2, we estimate the edge wavelengths to be:

$$\lambda_1 \approx 387\ nm; \qquad \lambda_2 \approx 211\ nm,$$

which yields $\lambda_0 \approx 299\ nm$, $\omega_0 \approx 6.30 \cdot 10^{15}\ s^{-1}$ and $\Gamma \approx 4.06 \cdot 10^{15}\ s^{-1}$. It should be noted that our typical operational wavelengths (λ) will always be longer than λ_0 (i.e., $\omega<\omega_0$), and hence δ will always be negative. Because of this assumption, the model will be invalid for positive δ.

We would also like to point out that in the case where the read-out is being done at a single frequency, the exact nature of the absorption mechanism is irrelevant. Given a measured absorption profile, the corresponding dispersion (i.e., index variation) is determined solely by the Kramers-Kronig relations [29] based on causality. In principle, this can be done by creating an array representing the imaginary part of the electric susceptibility corresponding to the measured absorption as a function of frequency, applying the Hilbert transform [29] to this array to find the corresponding values of the real part of the electric susceptibility, and then using this to determine the index as a function of frequency. However, such a numerical approach would be cumbersome to use in practice. A simpler alternative is to assume that the main peak in the absorption is due to a two-level system with a Lorentzian response. For such a two level system, the corresponding index variation can be written down analytically, in agreement with the result

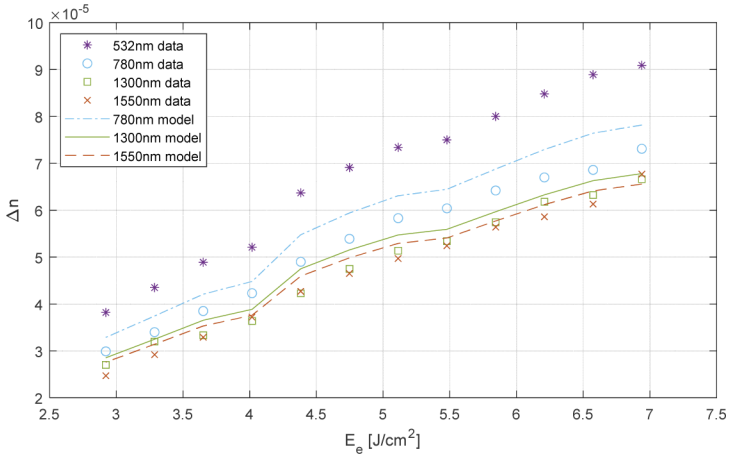

Fig. 3. E_e vs Δn for ~2mm thick PQ:PMMA holograms plotted alongside the $\Delta n(\lambda, \alpha)$ model. The markers correspond to Δn values calculated from the measured diffraction efficiency data using Eq. (9); purple stars: 532 nm, cyan circles: 780 nm, green squares: 1300 nm, and red crosses: 1550 nm. The lines were plotted by first obtaining α for each grating from the 532 nm data, and then calculating the expected Δn for the desired wavelength using Eq. (8) from the two level model; cyan dot-dash: 780 nm, green solid: 1300 nm, and red dashed: 1550 nm. Note that the data at 532 nm serve as reference and are assumed to correspond exactly to the theoretical model. The unslanted gratings were written at different locations on the same sample and the read beams were individually Bragg-matched for each measurement.

Optical Materials EXPRESS

obtained by applying the Hilbert transform. Of course, this approach entails the approximation that the absorption peak is Lorentzian; however, the small error produced by this approximation is not significant for experimental purposed. Finally, we note that this approach can be expanded to include additional peaks, by attributing these to individual two level transitions. As noted above, we have chosen not to do that here because one of the additional peaks is too narrow to influence the index at the wavelengths of interest, and the others are too small compared to the main peak. In the future, we will expand our studies to include these additional peaks and determine the degree to which they may influence the index at the wavelengths of interest.

3. Experimental comparison using Kogelnik's coupled wave equations

In the previous section, we found experimental values for ω_0 and Γ that we can use in Eq. (8) to get a wavelength dependent expression for Δn. To test this model, we must create multiple phase holograms with different values of Δn on the same sample and characterize them at various wavelengths, selecting one to be the 'reference' for calculating α. This can then be used to predict Δn at other wavelengths and to compare to our experimental data. The exposure energy density, E_e, can be changed by means of the exposure time in each consecutive hologram to generate distinct values of α, and thus Δn, for any given wavelength. However, Δn cannot be directly measured, but rather needs to be calculated from other parameters, as shown by Kogelnik [16]. The holograms were written to be of the transmission type, and all gratings were designed to be unslanted in order to minimize variables (i.e., both write beams have equal but opposite input angles with respect to the sample normal); the read beams are then individually Bragg matched at each measurement. Under these conditions, the value of Δn is given by [16]:

$$\Delta n = \frac{\lambda \cos(\theta)}{\pi\, d} \sin^{-1}\left(\sqrt{\eta_d}\right) \tag{9}$$

where d is the grating thickness, θ is the Bragg-matched angle inside the medium, and η_d is the diffraction efficiency. All of these parameters can be either fixed or measured directly; therefore, for any given read wavelength we can determine the experimental value of Δn. Figure 3 shows the results of one such set of holograms written at 532 nm and read at 532 nm, 780 nm, 1300 nm, and 1550 nm. The three values apart from the writing wavelength were chosen for being useful in a variety of applications: 780 nm is used in monocular passive ranging [10,20] as well as in rubidium based quantum sensors [30,31], and both 1300 nm and 1550 nm are used in telecommunications [8,10,19], among other areas. It should be noted that the expression in Eq. (9) assumes that the effect of any residual absorption is negligible. Since the wavelengths of interest for most applications are highly detuned from the resonant wavelength in our model, this assumption is reasonable.

The 532 nm data was chosen as a reference for calculating α. Figure 3 shows good agreement between our model and the experimental data, exhibiting an average error of 8.9%, 5.7%, and 5.5% at 780 nm, 1300 nm, and 1550 nm, respectively. Figure 4 shows a scatter plot of the model vs the data.

From Fig. 4 it is clear that there is an almost linear relationship between the model and data. Ideally, the lines would have unity slopes if the model generates perfect predictions. In reality, however, the interpolated slopes are 0.927 for 780 nm, 0.991 for 1300 nm, and 1.033 for 1550 nm – yielding R^2 values of 0.9956, 0.9903, and 0.9876, respectively, which were calculated as the square of the Pearson product. This shows that, while the model produces values that are close to the experimental data, there are still other factors that prevent it from yielding perfect results. There are three main sources of error that we have identified: the approximation of the electric susceptibility, the assumption that the absorption spectrum for any sample is equal to that of the reference sample, and the fact that Δn cannot be measured directly and so must be calculated using Eq. (9). The first source of error could potentially be improved by using

Optical Materials EXPRESS

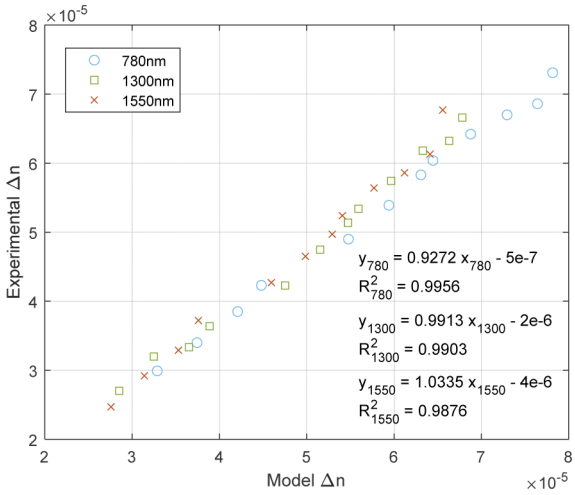

Fig. 4. Model vs Experimental Δn for the data corresponding to Fig. 3. The model was constructed by first obtaining α for each grating from the 532 nm data, and then calculating the expected Δn for 780 nm, 1300 nm, and 1550 nm using Eq. (8). Cyan circles: 780 nm, green squares: 1300 nm, and red crosses: 1550 nm. The equations for the corresponding linear trendlines are also shown.

a more complex model for the electric susceptibility, but this is hindered by the difficulty in measuring the absorption of the material below ~190 nm. The second source can be reduced through consistency in the manufacturing and evaluation processes. Finally, the third source depends on the precision with which the diffraction efficiency, Bragg angle, and thickness are measured. Uncertainty in these measurements directly results in additional uncertainty in the calculated value of Δn.

The model presented here provides a method for estimating the Δn of a sample at any given wavelength after measuring its characteristics at a single reference wavelength. Kogelnik's coupled wave equations relate the Δn of a holographic grating to its diffraction efficiency, but they do not predict how this modulation will vary by wavelength. Our Δn model based on a two-level approximation of the electric susceptibility takes into account the resonant frequency of the material (in this case PQ:PMMA) in order to fill this gap. By using both models in conjunction we may thus estimate the diffraction efficiency of any given sample at any given wavelength after measuring it at a reference wavelength. This drastically reduces the number of measurements -and thus the production time- required in order to characterize a sample for multi-wavelength applications like monocular passive ranging, telecommunications, spectroscopy, etc.

4. Conclusion

We have presented a model which permits the characterization of the Δn of any particular PQ:PMMA sample over a broad spectrum with only a small set of data at one reference wavelength. This can be used in conjunction with Kogelnik's well-known equations to also characterize the diffraction efficiency for any given wavelength. The parameters of the developed model were obtained from a new set of UV-VIS-NIR absorption measurements which agree with those presented by other authors. Employing the presented Δn model, it is possible to design PQ:PMMA phase holograms that operate over an extensive range of the optical spectrum, which are useful for many applications. One example would be a free space optical communication (FSOC) system. In general, FSOCs are implemented in situations where wired systems are impractical and broadcasting may be undesirable, such as in military outposts. The main

Optical Materials EXPRESS

advantage is that the signal can only be intercepted along a very narrow path, which itself can be monitored for added security. The bandwidth for such a system can be enhanced significantly via a WDM employing spatially superimposed gratings in PQ:PMMA. Understanding the behavior of the refractive index modulation at the desired wavelengths allows multiple channels to be designed on the same sample and operate anywhere from the near-infrared to the short-wave infrared. This may also prove useful for monocular passive ranging where only a subset of specific wavelengths must be precisely monitored [20,21].

The predictions of this model agree well with experimental data for wavelengths ranging from 532 nm to 1550 nm. Based on this finding, it is expected that the model would work well for virtually all wavelengths for which absorption can be neglected. As such, this model is expected to be highly useful in designing thick holographic gratings for a broad range of applications.

Funding. Naval Air Systems Command (N68335-19-C-0874, N68335-20-C-0842); Air Force Office of Scientific Research (FA9550-18-01-0359).

Acknowledgements. We acknowledge the use of the resources of the Keck Biophysics Facility, supported by the NCI CCSG P30 CA060553 grant awarded to the Robert H Lurie Comprehensive Cancer Center of Northwestern University.

Disclosures. The authors declare no conflict of interest.

Data Availability. Data underlying the results presented in this paper are not publicly available at this time but may be obtained from the authors upon reasonable request.

References

1. F. H. Mok, "Angle-multiplexed storage of 5000 holograms in lithium niobate," Opt. Lett. **18**(11), 915 (1993).
2. A. Yariv, S. S. Orlov, and G. A. Rakuljic, "Holographic storage dynamics in lithium niobate: theory and experiment," J. Opt. Soc. Am. B **13**(11), 2513 (1996).
3. J. Ashley, M.-P. Bernal, G. W. Burr, H. Coufal, H. Guenther, J. A. Hoffnagle, C. M. Jefferson, B. Marcus, R. M. Macfarlane, R. M. Shelby, and G. T. Sincerbox, "Holographic Data Storage," IBM J. Res. & Dev. **44**(3), 341–368 (2000).
4. Y. Hsiao, W.-T. Whang, and S. Lin, "Analyses on physical mechanism of holographic recording in phenanthrenequinone-doped poly(methyl methacrylate) hybrid materials," Opt. Eng. **43**(9), 1993–2002 (2004).
5. G. Beadie, M. Brindza, R. A. Flynn, A. Rosenberg, and J. S. Shirk, "Refractive index measurements of poly(methyl methacrylate) (PMMA) from 04–16 μm," Appl. Opt. **54**(31), F139 (2015).
6. Y. Luo, J. M. Russo, R. K. Kostuk, and G. Barbastathis, "Silicon oxide nanoparticles doped PQ-PMMA for volume holographic imaging filters," Opt. Lett. **35**(8), 1269 (2010).
7. Y. Luo, P. J. Gelsinger, J. K. Barton, G. Barbastathis, and R. K. Kostuk, "Optimization of multiplexed holographic gratings in PQ-PMMA for spectral-spatial imaging filters," Opt. Lett. **33**(6), 566 (2008).
8. O. Beyer, I. Nee, F. Havermeyer, and K. Buse, "Holographic recording of Bragg gratings for wavelength division multiplexing in doped and partially polymerized poly(methyl methacrylate)," Appl. Opt. **42**(1), 30 (2003).
9. G. J. Steckman, I. Solomatine, G. Zhou, and D. Psaltis, "Characterization of phenanthrenequinone-doped poly(methyl methacrylate) for holographic memory," Opt. Lett. **23**(16), 1310 (1998).
10. J. Gamboa, J. Vonckx, M. Fouda, and S. M. Shahriar, "PQ:PMMA holographic wavelength division multiplexing filters for use in monocular passive ranging and free space optical communications," in *Frontiers in Optics / Laser Science* (OSA, 2020), p. FW7A.1.
11. J. Gamboa, M. Fouda, and S. M. Shahriar, "Demonstration of shift, scale, and rotation invariant target recognition using the hybrid opto-electronic correlator," Opt. Express **27**(12), 16507 (2019).
12. A. Heifetz, J. T. Shen, J.-K. Lee, and M. S. Shahriar, "Translation-invariant object recognition system using an optical correlator and a super-parallel holographic random access memory," Opt. Eng. **45**(2), 025201 (2006).
13. J. Gamboa, T. Hamidfar, and S. M. Shahriar, "Integration of a PQ:PMMA holographic memory device into the hybrid optoelectronic correlator for shift, rotation, and scale invariant target recognition," Submitted for Publication (2021).
14. B. J. Shih, C. W. Chen, Y. H. Hsieh, T. Y. Chung, and S. H. Lin, "Modeling the diffraction efficiency of reflective-type PQ-PMMA VBG using simplified rate equations," IEEE Photonics J. **10**(6), 1–7 (2018).
15. C.-H. Lin, S.-L. Cho, S.-H. Lin, S. Chi, and K.-Y. Hsu, "Two-wavelength holographic recording in photopolymer using four-energy-level system: experiments and modeling," Opt. Eng. **53**(11), 112303 (2014).
16. H. Kogelnik, "Coupled wave theory for thick hologram gratings," Bell Syst. Tech. J. **48**(9), 2909–2947 (1969).
17. A. Heifetz, J. T. Shen, S. C. Tseng, G. S. Pati, J. K. Lee, and M. S. Shahriar, "Angular directivity of diffracted wave in Bragg-mismatched readout of volume holographic gratings," Opt. Commun. **280**(2), 311–316 (2007).
18. A. Pu, K. Curtis, and D. Psaltis, "Exposure schedule for multiplexing holograms in photopolymer films," Opt. Eng. **35**(10), 2824 (1996).

Optical Materials EXPRESS

19. A. Sato and R. K. Kostuk, "Holographic grating for dense wavelength division optical filters at 1550 nm using phenanthrenquinone-doped poly(methyl methacrylate)," in *Proc. SPIE 5216, Organic Holographic Materials and Applications*, K. Meerholz, ed. (2003), Vol. 5216, p. 44.
20. M. R. Hawks, R. A. Vincent, J. Martin, and G. P. Perram, "Short-range demonstrations of monocular passive ranging using O2 (X3Σg → b1 g +) absorption spectra," Appl. Spectrosc. **67**(5), 513–519 (2013).
21. H. Yu, B. Liu, Z. Yan, and Y. Zhang, "Passive ranging using a filter-based non-imaging method based on oxygen absorption," Appl. Opt. **56**(28), 7803 (2017).
22. J. Gamboa, T. Hamidfar, J. Vonckx, M. Fouda, and S. M. Shahriar, "Thick PQ:PMMA transmission holograms for free space optical communication via wavelength division multiplexing," Appl. Opt. **60**(28), 8851 (2021).
23. Y. Luo, S. B. Oh, and G. Barbastathis, "Wavelength-coded multifocal microscopy," Opt. Lett. **35**(5), 781 (2010).
24. S. Vyas, Y.-H. Chia, and Y. Luo, "Volume holographic spatial-spectral imaging systems [Invited]," J. Opt. Soc. Am. A **36**(2), A47 (2019).
25. L. Allen and J. H. Eberly, *Optical Resonance and Two-Level Atoms* (Dover Books on Physics, 1975).
26. M. S. Shahriar, Y. Wang, S. Krishnamurthy, Y. Tu, G. S. Pati, and S. Tseng, "Evolution of an N -level system via automated vectorization of the Liouville equations and application to optically controlled polarization rotation," J. Mod. Opt. **61**(4), 351–367 (2014).
27. R. W. Boyd, *Nonlinear Optics* (Academic Press, 2020).
28. T. Chung, W.-T. Hsu, Y.-H. Hsieh, and B.-J. Shih, "Recording 2nd order PQ:PMMA reflective VBG for diode laser output spectrum narrowing," Opt. Express **27**(6), 8258 (2019).
29. H. N. Yum and M. S. Shahriar, "Pump-probe model for the Kramers-Kronig relations in a laser," J. Opt. **12**(10), 104018 (2010).
30. Z. Zhou, M. Zhou, and S. M. Shahriar, "A superluminal Raman laser with enhanced cavity length sensitivity," *2019 Conf. Lasers Electro-Optics, CLEO 2019 - Proc. 27*, 29738–29745 (2019).
31. R. Newell, J. Sebby, and T. G. Walker, "Dense atom clouds in a holographic atom trap," Opt. Lett. **28**(14), 1266 (2003).